Environmental Toxicology and Pharmacology 104 (2023) 104298

Contents lists available at ScienceDirect

Environmental Toxicology and Pharmacology

journal homepage: www.elsevier.com/locate/etap

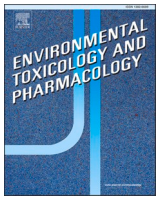

Nanoplastics activate a TLR4/p38-mediated pro-inflammatory response in human intestinal and mouse microglia cells

Joana Antunes [a,*], Paula Sobral [a], Marta Martins [a,*], Vasco Branco [b,c,**]

[a] MARE, Marine and Environmental Sciences Centre & ARNET, Aquatic Research Network Associated Laboratory, Department of Science and Environmental Engineering, NOVA School of Science and Technology (FCT NOVA), University NOVA of Lisbon, Caparica 2829-516, Portugal
[b] Research Institute for Medicines (iMed.ULisboa), Faculty of Pharmacy, Universidade de Lisboa, Av. Prof. Gama Pinto, 1649-003 Lisboa, Portugal
[c] Egas Moniz Center for Interdisciplinary Research (CiiEM), Egas Moniz School of Health & Science, Quinta da Granja, Monte de Caparica, 2829-511 Caparica, Portugal

ARTICLE INFO

Dr. M.D. Coleman

Keywords:
Nanoplastics
Intestine
Inflammation
TLR4
Microglia
p38

ABSTRACT

The crescent presence of nanoplastics in the environment raises concerns regarding their potential impact on health. This study exposed human colon adenocarcinoma cells (HT29) and microglia cells (N9) to nanoplastics (25 nm, 50 nm, and 100 nm Polystyrene) to investigate their inflammatory responses, which are vital for body's defence. Although cytotoxicity remained generally low, HT29 cells exhibited a notable upregulation of p50 and p38 expression, concomitant with elevated TLR4 expression, in contrast with N9 cells that showed a less pronounced upregulation of these proteins. Additionally, nanoplastic exposure increased IL-1ß levels, partially attenuated by pre-exposure to TLR4 or p38 inhibitors. Intriguingly, N9 cells exposed to nanoplastics exhibited substantial increases in iNOS mRNA. This effect was entirely prevented by pre-exposure to TLR4 or p38 inhibitors, while TNF-α mRNA levels remained relatively stable. These findings underscore the potential of nanoplastics to activate inflammatory pathways, with response kinetics varying depending on the cell type.

1. Introduction

The overuse and inadequate disposal of plastic polymers has led to a serious pollution problem at the global scale. Polystyrene is one of the most widely used plastic polymers (15.61 million metric tons produced in 2021 and PS), with applications in packaging, insulation, consumer goods, electronics, and construction (Bonanomi et al., 2022). This material is lightweight and easily breakable into smaller particles, thus posing a threat to animal and human health (Palmer and Herat, 2021). It is therefore unsurprisingly one of the most commonly found materials in the environment, particularly in marine ecosystems (Pabortsava and Lampitt, 2020), which makes it an important polymer to study.

Of the many environmental challenges posed by plastic particles released by anthropogenic activities (PlasticsEurope, 2022), degradation into nanoparticles by ultraviolet radiation, mechanical abrasion, or biological mechanisms (Mattsson et al., 2015) to an unknown nanoscale limit (El Hadri et al., 2020) is particularly concerning. Nanoplastics (NP; diameter < 100 nm) are among the least studied despite their potentially high risk to human health, which adds to the lack of standardized methodologies to assess their levels in the environment and biota (European Commission, 2022).

Due to their small size and the ability to cross biological membranes (Kihara et al., 2021), NP can be easily ingested (Botterell et al., 2019), bioaccumulate, and biomagnified (He et al., 2020). Nanoplastic uptake has been associated with oxidative stress (Zhou et al., 2023) and tissue damage (Larue et al., 2021), metabolic changes (Du et al., 2022; Haldar et al., 2023), changes to the function of both membranes and cells (Han et al., 2024), reduction in reproductive success (Jewett et al., 2022), behavioural disturbances (Ferreira et al., 2023) malformations and changes in feeding ability in fish (Teles et al., 2020). Also, evidence of dermal uptake has been reported (Llorca and Farré, 2021; Ragnarsdóttir et al., 2022; Revel et al., 2018).

Nanoplastics may potentially interfere with intestinal membrane receptors and intracellular inflammatory signalling cascades (Bouwmeester et al., 2015; Yee et al., 2021), inducing immune cells to release cytokines thus triggering inflammation (S. Han et al., 2020; Hwang et al., 2020). Reported outcomes include microbiota alterations, intestinal barrier permeability, oxidative stress, inflammation, neurotoxicity,

* Corresponding authors.
** Corresponding author at: Research Institute for Medicines (iMed.ULisboa), Faculty of Pharmacy, Universidade de Lisboa, Av. Prof. Gama Pinto, 1649-003 Lisboa, Portugal.
E-mail addresses: jcsantunes@fct.unl.pt (J. Antunes), marta.martins@fct.unl.pt (M. Martins), vasco.branco@ff.ulisboa.pt (V. Branco).

https://doi.org/10.1016/j.etap.2023.104298
Received 10 April 2023; Received in revised form 5 October 2023; Accepted 17 October 2023
Available online 19 October 2023

and behavioural disturbances (Aljabali et al., 2023). However, the underlying mechanisms are poorly understood. This is especially true for gut cells which are the primary site of contact for NP after oral ingestion. As the gastrointestinal tract is very important in maintaining immune homeostasis, (Vezza et al., 2016), the imbalance of inflammatory processes and cytokine secretion (e.g. TNF-α and IL-1β) may be linked to disruption of the epithelial-cell barrier which can lead to inflammation and dysregulation of mucosal homeostasis (Oliveira et al., 2022).

Toll-like receptors (TLRs) are membrane proteins that belong to the pattern recognition receptor (PRR) family and play an important role in recognizing invading pathogens and triggering an immediate immune response. Activation of TLRs also leads to the synthesis of pro-inflammatory cytokines and chemokines (Liu et al., 2017; Zbinden-Foncea et al., 2012). Specifically, TLR4 recognizes bacterial lipopolysaccharide (LPS), the major component of membranes of Gram-negative bacteria (Poltorak et al., 1998) leading to a canonical activation of the NF-kB pathway and p38 (Sharif et al., 2007); Wang et al. (2018)). The latter is strongly activated by stress and plays an important role in immune responses, such as activation and regulation of kinases, and interaction with other signalling pathways, as well as regulation of cell survival and differentiation (Whitaker and Cook, 2021). This factor is also important in producing cytokines and in return is also strongly activated by proinflammatory cytokines such as interleukin 1 (IL-1ß) and tumour necrosis factor a (TNF-α), which play an important role in regulating the inflammatory response (Cuadrado and Nebreda, 2010).

Therefore, we hypothesized that exposure of cells to nanoplastic particles triggers inflammatory signalling via the NF-kB and/or p38 MAPK pathways. To test this hypothesis, we exposed human colorectal adenocarcinoma cells (HT29 cells) and mouse microglia cells (N9 cells) to different concentrations and sizes of polystyrene nanoplastics in the presence or absence of either a TLR4 or p38 inhibitor and investigated NF-kB and p38 activation, TLR4 expression and the levels of pro-inflammatory gene transcripts.

2. Material and methods

2.1. Nanoplastics

Polystyrene fluorescent nanospheres (hereafter NP), with 25, 50 and 100 nm diameter and a density of 1.05 $g.cm^{-3}$ from Thermo Scientific, were purchased from Distrilab, Netherlands (catalog references, G25, G50 and G100, respectively. https://distrilab.nl/dyed-and-fluorescent-particles/). Fluorescent dyes are incorporated into the polymer mix (not surfaced dyed) and the NP were packaged in deionized water with trace amounts (<0.1%) of surfactant (Triton-X 100) and preservative (sodium azide) to inhibit aggregation and promote stability.

2.2. Nanoplastic size and potential zeta

Size and zeta potential of NP were analysed with an HORIBA nanoparticle analyser SZ-100. At least three replicates of a NP solution (500 $\mu g.mL^{-1}$) diluted in either PBS or culture medium were analysed.

2.3. Cell culture

Human colorectal adenocarcinoma cells (HT29; ATCC, USA) were cultured at 37ºC in Dulbecco's Modified Eagle medium with high glucose (4.5 g/L), with GlutaMAX and no sodium pyruvate, (Gibco), 10% of heat-inactivated foetal bovine serum (FBS) (Biochrome) and 1% penicillin/streptomycin (100 $units.mL^{-1}$ of penicillin and 100 $\mu g.mL^{-1}$ of streptomycin) (Gibco) in a humidified incubator with a 5% CO_2 atmosphere. N9 mouse microglia were a kind gift from Professor Dora Brites (iMed.ULisboa) and were cultured in RPMI medium (Gibco), 10% of FBS (Biochrome) and 1% penicillin/streptomycin (100 $units.mL^{-1}$ of penicillin and 100 $\mu g.mL^{-1}$ of streptomycin) (Gibco) in a humidified incubator with 5% CO_2 atmosphere at 37ºC.

Cells were seeded at 1.0×10^6 cells per 75 cm^2 culture flask. Culture medium was changed every two days after seeding and cells were harvested after reaching 80% confluency using 0.05% trypsin/EDTA (Sigma).

2.4. Cell viability assay

Cell viability was determined by the MTT ((3–4,5-dimethylthiazol-2-yl) – 2,5 – diphenyltetrazolium bromide) assay described by Carvalho et al. (2008). Cells (5×10^3 cells per well) were cultured in 96-well plates and allowed to attach for 24 h before the addition of NP (0, 25, 50, 100, 250 and 500 $\mu g.mL^{-1}$). Cells exposed to Triton-X 100 (10%) were used as a positive control. After 24, 48 and 72 h of exposure, MTT was added to plates at a final concentration of 400 $\mu g.mL^{-1}$ per well followed by incubation at 37 ºC for 2 h. Following the incubation period, the MTT solution was removed, and the formazan crystals were dissolved with 4:1 dimethyl sulfoxide/glycine buffer (pH 10.5) (Honeywell, UK). The absorbance was measured at 550 nm and the cellular viability was calculated relatively to the control group.

2.5. Exposure of cells to nanoplastics

HT29 and N9 cells were seeded in 10 mm^2 culture dishes (1×10^6 cells per plate) and allowed to reach 70–80% confluence. Afterwards, culture medium was replenished and cells were exposed to 25 and 500 $\mu g.mL^{-1}$ of NP (25, 50 and 100 nm) for 24 h. Lipopolysaccharide (LPS) (Sigma-Aldrich) (300 $ng.mL^{-1}$) was used as positive control. After exposure, cells were rinsed with PBS and detached from plates with trypsin. The cellular pellet was collected by centrifugation (5 min at 600 g) and washed with PBS (Lonza, BioWhittaker, USA). Following a second centrifugation, the pellet was resuspended in the appropriate lysis buffer, depending on the requirements of each specific protocol (see below).

2.6. Total cell lysates

Cell lysates were obtained by disrupting cellular pellets in lysis buffer (25 mM Tris–Cl, pH 7.5; 100 mM NaCl; 2.5 mM EDTA; 2.5 mM EGTA; 20 mM NaF, 1 mM sodium orthovanadate, 20 mM sodium pyrophosphate; 20 mM sodium β-glycerophosphate; 0.5% Triton X-100; and 1 tablet of protease inhibitor cocktail (Roche) per 10 mL). After lysis, samples were frozen at − 20 ºC until subsequent analysis.

2.7. Nuclear cell fraction

Following exposure to NP (25 and 500 $\mu g.mL^{-1}$ of 25, 50 and 100 nm NP) and LPS (300 $ng.mL^{-1}$) for 24 h, cells were washed twice with versene, resuspended in buffer A (10 mM HEPES pH 7.9, 1.5 mM $MgCl_2$, 10 mM, protease inhibitor tablets - 1 per 10 mL) and incubated on ice for 15 min. Afterwards, Triton X-100 (0.5%) was added, and the lysate was mixed by vortex for 10 s. Samples were centrifugated at 6500 g for 20 s and the cytosolic supernatant was removed. The pellet was washed with 150 μL of buffer A (without Triton) and centrifuged again at 6500 g for 20 s and the supernatant discarded. A volume of 100 μL of buffer B (HEPES pH 7.9, 1.5 mM $MgCl_2$, 420 mM NaCl, 0.2 mM EDTA, 25% v/v Glycerol, protease inhibitor tablets - 1 per 10 mL) was added to samples to resuspend the pellet. Samples were incubated on ice with vigorous stirring (using a magnetic bar) for 30 min. Nuclear extracts (supernatants) were recovered after a final 10 min centrifugation at 13,000 g and 4 ºC.

2.8. Total protein quantification

The total protein content was determined in the soluble fraction of each lysate, using the Bradford method (Branco et al., 2022). After

mixing diluted (5x) Coomassie dye (BioRad) with each sample (96-well plates), the absorbance was measured at 595 nm in a microplate reader (Zenyth 3100, Anthos Labtec Instruments). The protein concentration was calculated from a calibration curve (1 – 12 μg of protein per μL) using bovine serum albumin (BSA) (Sigma-Aldrich) as a standard.

2.9. Determination of protein expression levels of p50 NF-Kβ subunit, p38 and TLR4

To evaluate protein expression of p50 NF-Kβ subunit and p38, total cellular lysates and nuclear fractions of cells were analysed by Western Blot, after 24 h of NP exposure. Protein expression was analysed after separation of total soluble proteins (40 μg) by SDS–PAGE on a 4–12% Bis–Tris gel (Invitrogen, ThermoFisher Scientific, USA) with MES running buffer under reducing conditions (140 v for 1 h). Proteins were subsequently transferred (40 v for 7 min) to a nitrocellulose membrane using the iBlot 2 dry blotting system (Invitrogen), blocked with a 5% skimmed milk solution (1 h) and rinsed with PBST. Afterwards, membranes were incubated with primary and secondary antibodies for the proteins of interest and detected with chemiluminescence using the Biorad Chemidoc System. Membranes were submerged with shaking for 1 h in a 1% BSA solution containing the respective primary antibody (1/1000). The following antibodies were used: NF-Kβ p50 (sc-166588, Santa Cruz), p38 (sc-13666588, Santa Cruz). For TLR4 expression, TLR4 Antibody (25): sc-293072 was used (Santa Cruz Biotechnology Inc).

Expression levels were normalized for protein loading on the gel, which was assessed by Ponceau S (Sigma-Aldrich).

2.10. Pro-inflammatory gene transcription (qRT-PCR)

Cells (HT29 and N9 cells) were seeded in 6-well plates (1×10^5 cells per well) and exposed to 25 and 500 $\mu g.mL^{-1}$ of NP (25, 50 and 100 nm) and LPS (300 $ng.mL^{-1}$), as a positive control. Additionally, parallel assays, were performed encompassing either pre-exposure (24 h) of cells to 5 μM of a TLR4 inhibitor (TAK-242 - CAS 243984–11–4 – Calbiochem) or pre-exposure to 10 μM of a p38 inhibitor (SB2399063, Sigma-Aldrich). After pre-exposure, medium was changed, and cells exposed to NP as mentioned above.

RNA extraction was performed using an NZY Total RNA Isolation kit (NZYTech, Portugal) according to manufacturer instructions. Total RNA concentration was determined from spectrophotometric optical density measurement (260 and 280 nm). For each sample tested, the ratio between the spectrophotometric readings at 260 nm and 280 nm (OD_{260}/OD_{280}) was used to evaluate RNA purity, with the ratio ranging between 1.87 and 2.04 for all samples.

cDNA was synthesized using a NZY First-Strand cDNA Synthesis Kit (NZYTech, Portugal) using 1 μg of RNA as template. Gene expression quantification was performed using NZY qPCR Green Master Mix (NZYTech, Portugal) with 4 μM forward primer and 4 μM reverse primer and 100 ng of template cDNA in a 10 μL reaction volume. All samples were run in triplicate and the output level was reported as the average of the 3 measurements. Amplification conditions included 2 min at 50 °C and 10 min at 95 °C, and then 40 cycles at 95 °C for 15 s and 60 °C for 1 min on a Applied Biosystems QuantStudio™ 7 Flex Real-Time PCR System (Applied Biosystems, Foster City, CA, USA).

The primer sequences for human and mouse IL-1β, iNOS, TNF-α and GAPDH (Supplementary Table 1) were designed with Primer-Blast and synthesis was performed by StabVida (https://www.stabvida.com). After RT-PCR gene levels were calculated by the relative quantification $2^{-\Delta\Delta CT}$ method (Livak and Schmittgen, 2001), using GAPDH as the housekeeping gene.

2.11. Statistical analysis

Data in Figures are represented as the mean ± standard deviation (S.D).

Statistical analyses were conducted using GraphPad version 10.0.2. Data normality was evaluated by the Shapiro-Wilks test and variance homogeneity using Spearman's test for heteroscedasticity. When appropriate, data were log-transformed to comply with assumptions of parametric tests.

Significance of main and interaction effects was evaluated by a Two-Way ANOVA (see Supplementary table 2 for details), followed by post-hoc assessment with a Tukey test (see Supplementary Table 3 for details) to evaluate differences between exposure groups. When appropriate, data were log-transformed to comply with assumptions of parametric tests. Differences between groups were classified as significant at $p < 0.05$ and considered very significant at $p < 0.01$.

3. Results

3.1. Effect of NP exposure on viability of HT29 and N9 cells

The viability of HT29 and N9 cells after 24, 48, and 72 h of NP exposure is presented in Fig. 1. In general, the viability of HT29 was > 80% with no significant differences resulting from increased levels of exposure to 25 and 50 nm (25 nm: Two-way ANOVA, F (df, 2, 56) = 1.257, p = 0.2924; 50 nm: Two-way ANOVA, F (df, 2, 52) = 1.372, p = 0.2626). Although a concentration related effect was observed for the 100 nm (Two-way ANOVA, F (df, 2, 53) = 8.825, p = 0.0005), pairwise post-hoc comparisons versus the non-treated group did not disclose significant differences (Tukey test, $p > 0.05$, supplementary Table 3).

Regarding N9 cells, viability decreased significantly with exposure denoting a concentration-related effect (25 nm: Two-way ANOVA, F (df, 2, 42) = 173.7, $p < 0.0001$; 50 nm: Two-way ANOVA, F (df, 2, 35) = 27.46, $p < 0.0001$; 100 nm: Two-way ANOVA, F (2, 43) = 3.594 P = 0.0360), with NP of 50 nm size causing the highest decrease in viability (>50% decrease). This was most evident after 48 h of exposure (Fig. 1).

3.2. p50 and p38 expression HT29 and N9 cells

Overall, no changes were observed in the total cellular expression of p50 and p38 following exposure to nanoplastics (data not shown). A significant increase in the nuclear translocation of p50 NF-kB relative to the control was observed in HT29 exposed to NP (Fig. 2) in a concentration-dependent effect (Two-way ANOVA, F(df, 2, 13)= 26,89 $p < 0.0001$), with cells exposed to 25 $\mu g.mL^{-1}$ of NP showing a higher up-regulation compared to the control, especially for the 25 nm NP (Tukey's test, q = 7.397, DF = 13, p = 0.0036; supplementary Table 3). An overall increase in the nuclear translocation of p38 (up-to 2-fold) was also observable in HT29 albeit the relation to concentration was marginally non-significant (Two-way ANOVA, F (df, 2, 12), p = 0.055).

In N9 cells, p50 and p38 translocation did not vary significantly compared to the control for any of the treatments (Tukey's test, $p > 0.05$, supplementary Table 3) (Fig. 2).

3.3. TLR4 expression in HT29 and N9 total cell lysates

Analysis of basal TLR4 expression showed that N9 cells expressed higher levels of this receptor compared to HT29 cells (Fig. 3A).

Despite the lower basal levels, HT29 showed an up-regulation of TLR4 of approximately 2-fold relative to the non-treated control when cells were exposed for 24 h to NP (Fig. 3B). This increase was related to concentration (Two-way ANOVA, F(df, 2, 9) = 23,02, p = 0.0003) and denoted a significant interaction with size (Two-way ANOVA, F(df, 4, 9) = 8807 p = 0.0035). Smaller NP (25 and 50 nm) increased TLR4 significantly at 25 $\mu g.mL^{-1}$ (25 nm: Tukey's test, q = 7.08, DF = 12, p = 0.0125; 50 nm: Tukey's test, q = 7.07, DF=12, p = 0.0126) whereas larger particles (100 nm) only at 500 $\mu g.mL^{-1}$ (Tukey's test, q = 6.662, DF = 12, p = 0.0183).

This up-regulation was not significant in N9 cells (Fig. 3B; Two-way

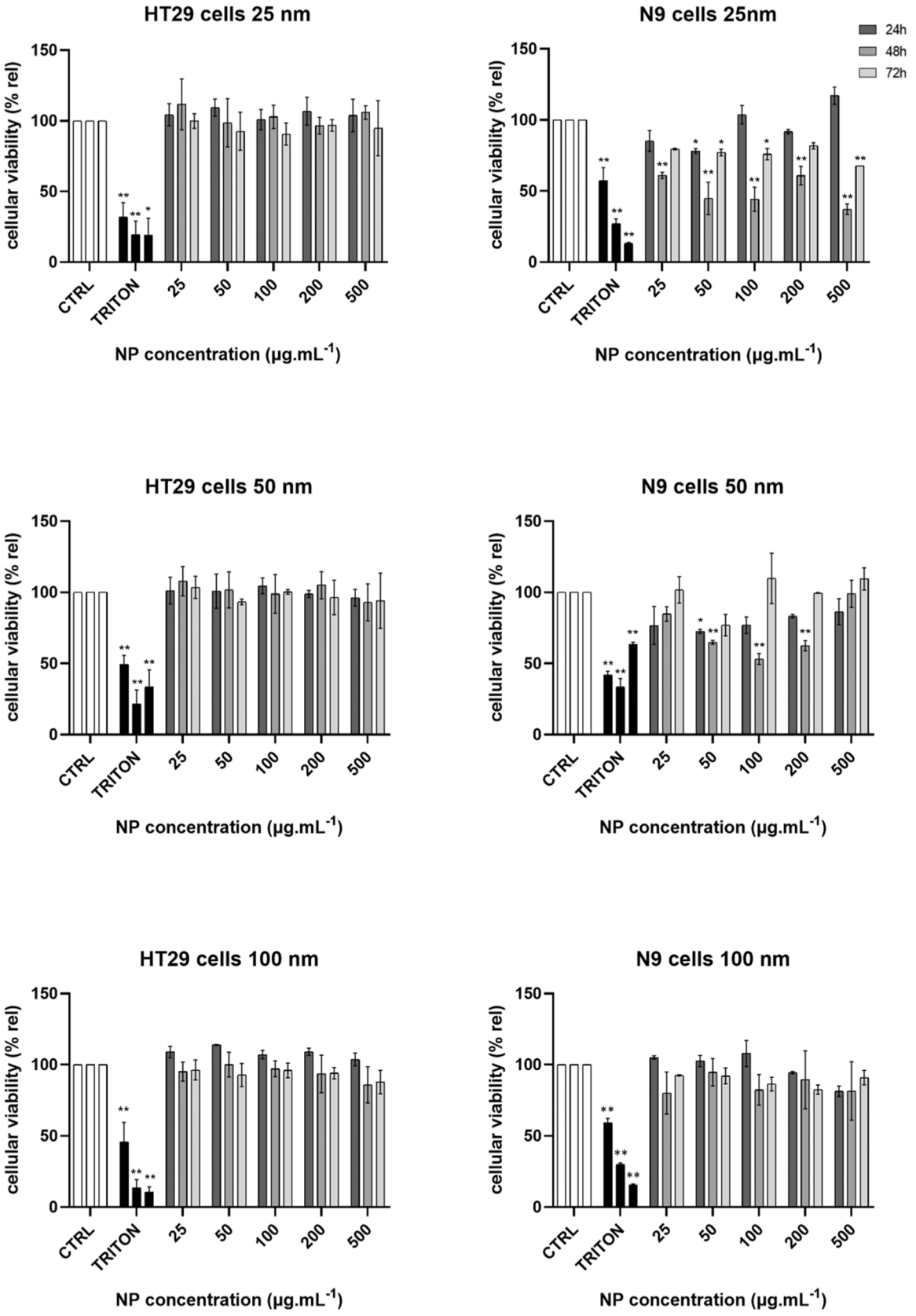

Fig. 1. Effect of polystyrene nanoplastics (NP) on the viability of human colon adenocarcinoma (HT29) and mouse microglia cells (N9), as measured by the MTT assay. Viability was analysed after exposure of cells to different concentrations (25, 50,100,200, 500 µg.mL^{-1}) and particles sizes (25, 50 and 100 nm) for 24, 48 and 72 h. Triton X-100 (10%) was used as a positive control. Results are represented as the mean ± S.D. of at least three independent experiments. Statistical testing was performed on log-transformed data * significantly different ($p < 0.05$) from the control; * * very significantly different ($p < 0.01$) from the control (Tukey's test).

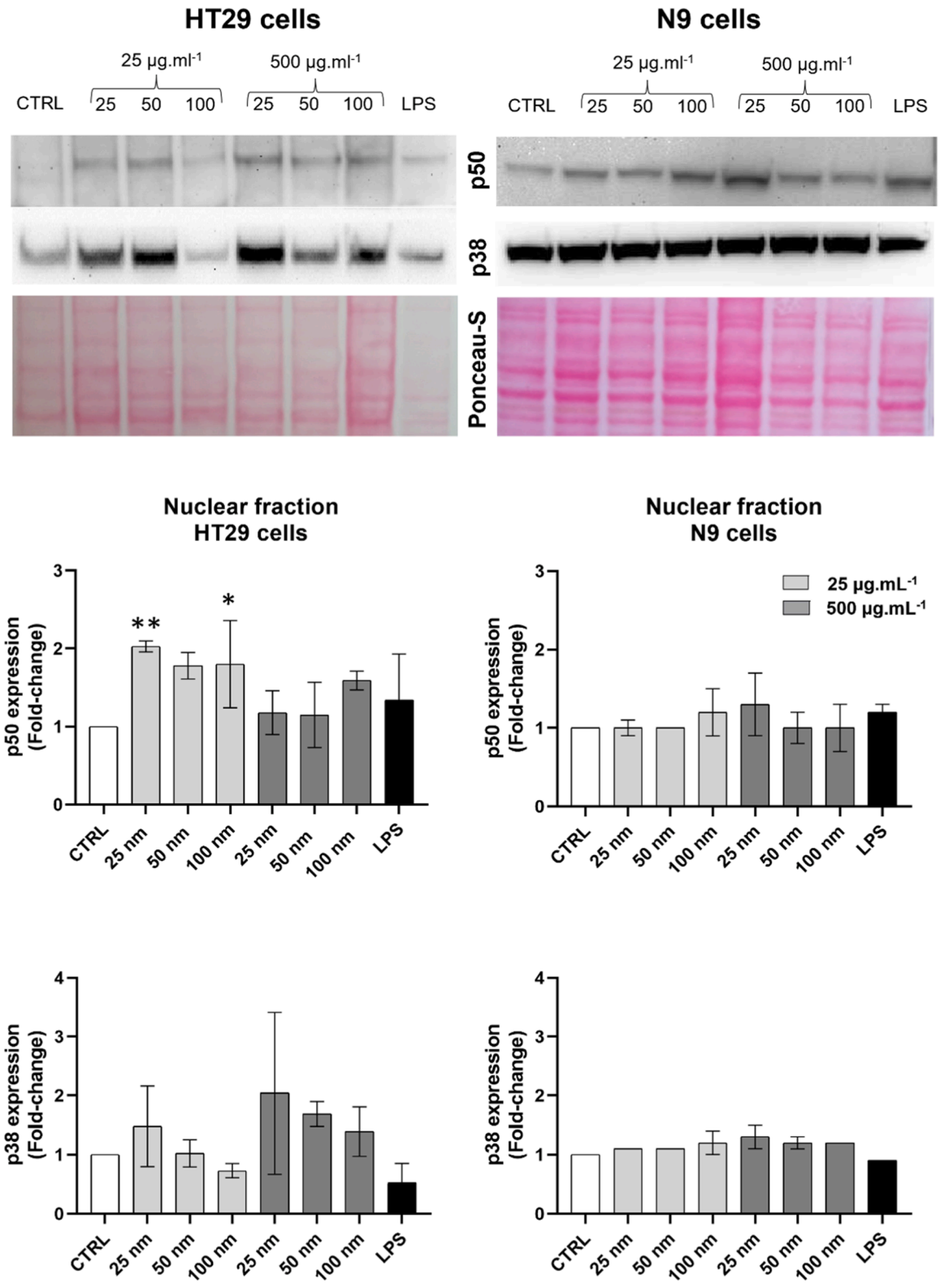

Fig. 2. p50 and p38 expression in the nuclear fraction of HT29 and N9 cells, as determined by Western Blot, after exposure to three different sizes of NP (25, 50 and 100 nm) in two different concentrations (25 and 500 µg.mL^{-1}) and LPS (300 ng.mL^{-1})for 24 h and LPS (300 ng.mL^{-1}). Results were normalized for protein loading using Ponceau-S staining. Statistical testing was performed on log-transformed data. Values are the mean ± S.D of three independent experiments. * significant differences with a $p < 0.05$ from control (Tukey's test).

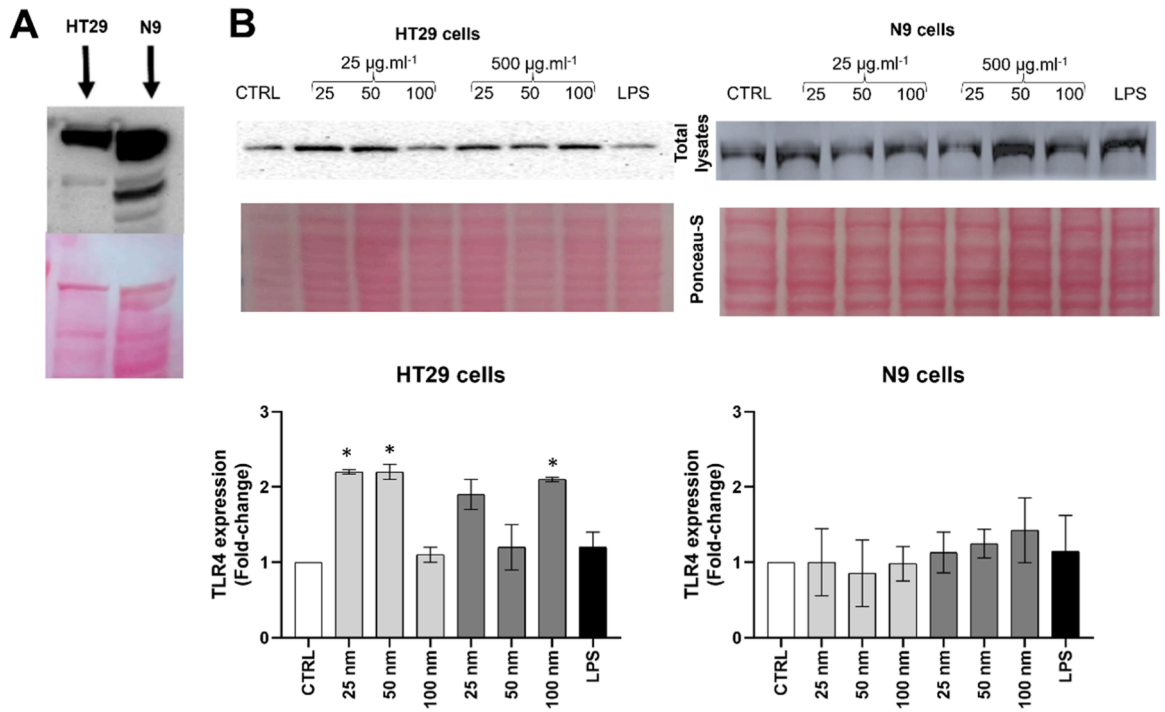

Fig. 3. A) Basal TLR4 expression in HT29 and N9 cells. B) TLR4 expression in HT29 and N9 cells exposed to 25, 50 and 100 nm NP at 25 and 500 µg.mL^{-1} and LPS (300 ng.mL^{-1}) for 24 h. Values are the mean ± S.D of three independent experiments. Statistical testing was performed on log-transformed data * significant differences with a $p < 0.05$ from control (Tukey's test).

ANOVA $p > 0.05$, Supplementary Table 2) which had already a high basal expression of TLR4 (Fig. 3A).

3.4. Effects of nanoplastics over pro-inflammatory gene expression

Effects of NP exposure in gene expression of HT29 and N9 cells are presented in Figs. 4 and 5, respectively.

The overall effect of particle size (Two-way ANOVA HT29: F (df, 2, 25) = 3.903, $p = 0.0335$; N9: SizeF (2, 16) = 6.031, $p = 0.0112$) and concentration (HT29: F(df, 2, 25) = 10.51, $p = 0.0005$; N9 F (df, 2, 16) = 28.50, $p < 0.0001$) over IL-1β mRNA was very significant in both cell lines (Figs. 4A and 5 A).

After 24 h of exposure to NP at 25 µg.mL^{-1}, IL-1β mRNA levels (Fig. 4A) were increased in HT29 cells exposed to 50 nm NP (Fig. 4A; Tukey's test, q = 6.172, DF = 25, $p = 0.051$). When pre-exposed to the TLR4 and p38 inhibitor IL-1β mRNA expression values of HT29 cells remained unchanged (Tukey's test, $p > 0.05$, Supplementary Table 3).

When NP concentration rose to 500 µg.mL^{-1} (Fig. 4 B), a significant increase in IL-1ß (3-fold) relative to the control was observed with exposure of HT29 cells to the smaller NP (25 nm) (Tukey's test, q = 5.314, DF = 25, $p = 0.0217$), which could be blocked by inhibiting TLR4 or p38.

Overall, exposure to NP at both 25 and 500 µgmL^{-1} caused no significant differences in iNOS mRNA levels in HT29 (Two-way ANOVA, F (df, 2, 25) = 0.9016, $p = 0.4187$) (Fig. 4C and D). It is noteworthy that when pre-exposed to the p38 inhibitor, iNOS transcription increased significantly in cells exposed to 50 nm-sized particles (Tukey's test, q = 6.298, DF = 13 $p = 0.0068$).

N9 cells showed a significant increase in IL-1β mRNA levels following 24 h of exposure to 25 µgmL^{-1} NP relative to the control for the 25 (Tukey's test, q=5.027, DF = 16, $p = 0.0503$) and 100 nm (Tukey's test, q = 10.18, DF = 16, $p < 0.0001$) sizes, (Fig. 5 A). Most interestingly, this increase was completely subdued when NP concentration rose to 500 µg.mL^{-1} (Fig. 5 B) denoting a significant interaction between size and concentration (Two-way ANOVA, F (df, 4, 16) = 7.810, $p = 0.0011$).

A very similar trend was observed for iNOS in N9 cells, again showing increased transcription following exposure to 25 µg.mL^{-1} (Fig. 5) (up to 25 fold with 100 nm NP), but not at 500 µg.mL^{-1} demonstrating a concentration-related effect (Two-way ANOVA, F (df, 2, 19) = 52.30, $p < 0.0001$). Most interestingly, in several cases pre-exposure of N9 cells to TLR4 and p38 inhibitors prevented up-regulation of IL-1β and iNOS transcription compared to N9 cells exposed only to NP (see supplementary Table 3 for Tukey test details) (Fig. 5A and C).

TNF-α expression values in HT29 cells were only significantly increased in cells exposed to 25 µg.mL^{-1} of 100 nm particles (Fig. 4E) (Tukey's test, q = 7.367, DF = 24, $p = 0.0007$). No clear effect of TLR4 or p38 inhibition was observed for all sizes and concentrations (Tukey's test, $p > 0.05$, Supplementary Table 3) (Fig. 4E and F).

Overall, no significant differences were registered in TNF-α levels (Fig. 5 E and F) values for N9 cells in any of the exposure conditions (Tukey's test, $p > 0.05$, Supplementary Table 3). An exception was observed for 50 nm NP at 500 µg.mL-1, where TNF-α levels (Fig. 4F) were significantly higher relative to the control (Tukey's test, q = 8.288, DF = 18, $p = 0.0004$), but only for the highest exposure concentration (500 µg.mL^{-1}) showing a significant interaction between the effect of particle size and concentration (Two-way ANOVA, F (df 4, 18) = 11.75, $p < 0.0001$).

Pre-exposure to the TLR4 inhibitor (Tukey's test, $p > 0.05$, supplementary table 3) did not change this effect, but pre-exposure to the p38 inhibitor significantly decreased TNF-α expression values for the 50 nm size (Tukey's test, q = 11.16, DF = 9, $p = 0.033$) (Fig. 5F).

4. Discussion

Our results showed that NP of different sizes and in a wide range of concentrations (25–500 µg.mL^{-1}) did not affect significantly the cellular viability of human colorectal adenocarcinoma cells (HT29) (Fig. 1). However, the viability of mouse microglial cells (N9 cells) was

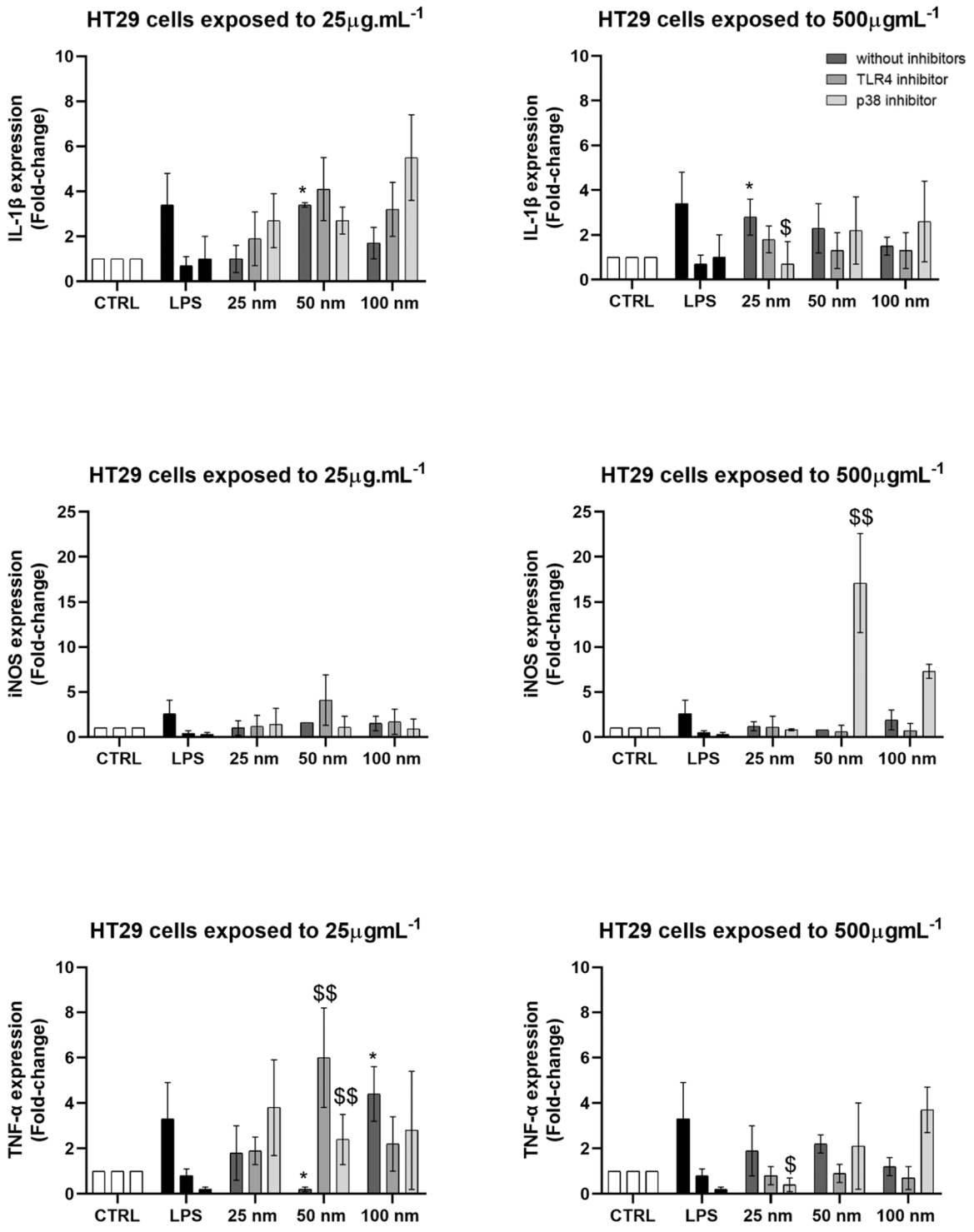

Fig. 4. HT29 cells mRNA expression for IL-1β (panels A and B), iNOS (panels C and D) and TNF-α (panels E and F) after 24 h of exposure to 25, 50 and 100 nm nanoplastics at 25 and 500 µg.mL^{-1} and LPS (300 ng.mL^{-1}). Data represent the mean ± S.D of at least 3 independent replicates. Statistical testing was performed on log-transformed data Tukey test: * significantly different from the control ($\rho < 0.05$); $ significantly different from the corresponding group without pre-exposure to either the TLR4 or p38 inhibitor ($p < 0.05$). Data represent the mean ± S.D of at least 3 independent replicates.

significantly hindered by exposure to NP, with MTT reduction decreasing to about 50% after 48 h of exposure. This effect was most evident for smaller size nanoplastics (25 and 50 nm) which is in line with previous reports using comparable exposure concentrations in other unicellular models such as microalgae (Hazeem et al., 2020), HepG2 cells (He et al., 2020), splenocytes (Li et al., 2022), neuronal cells (Jung et al., 2020).

The effect of nanoplastics on cellular viability is attributed to the easier internalization of smaller size particles (Kihara et al., 2021) which eventually causes cell death (Gopinath et al., 2019; Jung et al., 2020). However, differences in sensitivity between cell lines are often reported, for example between neuronal cells and astrocytes (Jung et al., 2020), which is also in line with the differences we observed between HT29 and N9 cells.

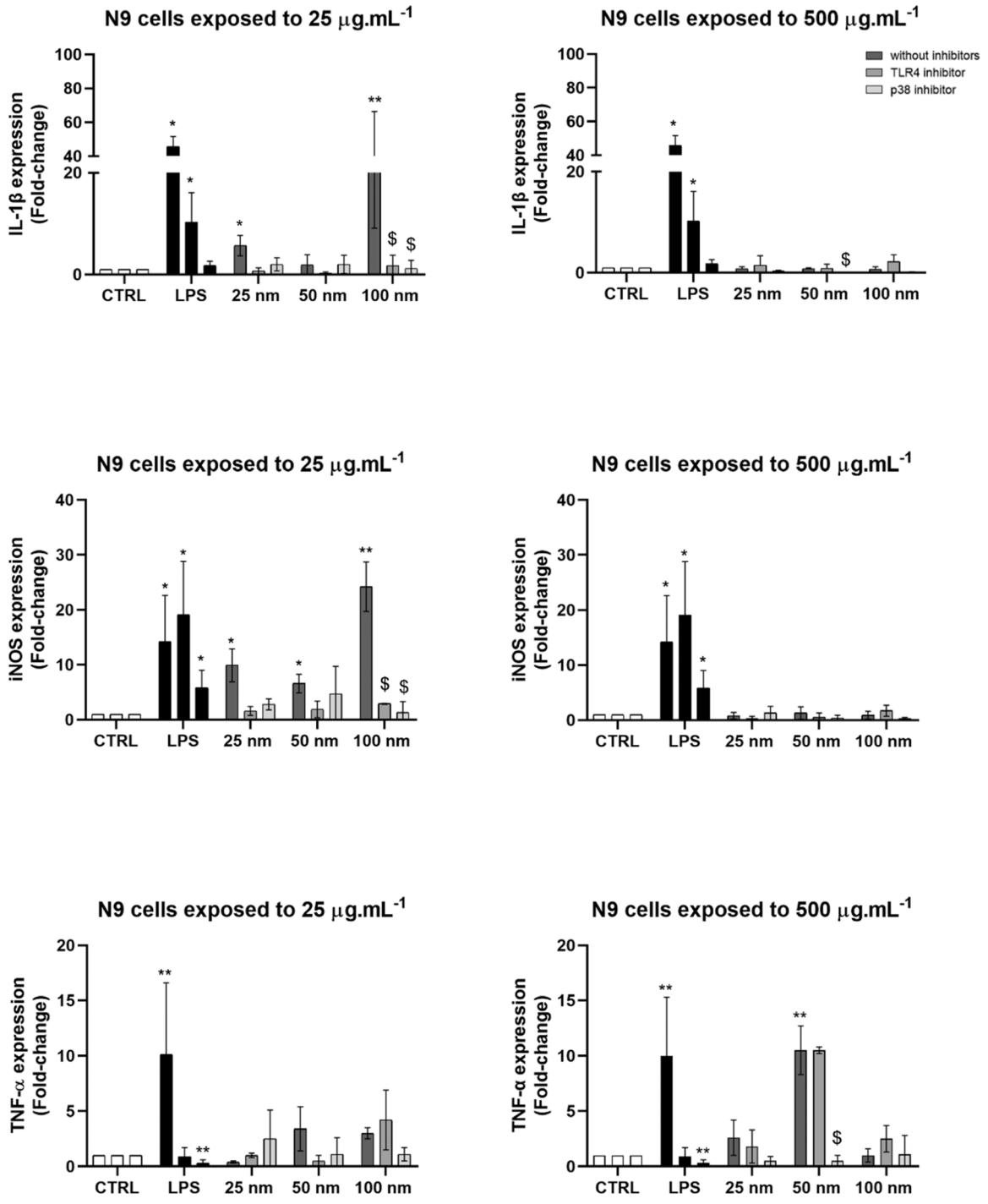

Fig. 5. N9 cells mRNA expression for IL-1β (Panels A and B), iNOS (Panels C and D) and TNF-α (Panels E and F) after 24 h of exposure to 25, 50 and 100 nm nanoplastics at 25 and 500 μg.mL^{-1} and LPS (300 ng.mL^{-1}). Data represent the mean ± S.D of at least 3 independent replicates. Statistical testing was performed on log-transformed data. Tukey test: * significantly different from the control ($\rho < 0.05$); $^{\$}$ significantly different from the corresponding group without pre-exposure to either the TLR4 or p38 inhibitor ($p < 0.05$). Data represent the mean ± S.D of at least 3 independent replicates.

Interestingly, Jung et al. (2020) reported that astrocytes, while not showing a decrease in viability, exhibited reactive astrogliosis as seen by an increase in lipocalin-2, showing that NP might induce changes to cellular metabolism regardless of their effect on cellular viability.

Indeed, we observed that HT29 cells upregulated the nuclear translocation of p50 and p38 after being exposed to smaller NP (Fig. 2), even though the overall expression was unchanged (data not shown).

NF-kB1 is present in the cytoplasm of cells as an inactive heterodimer (p50/p65) bound by IκBα, which prevents the transcription factor from migrating into the nucleus (Bacher et al., 2021). The activation of NF-kB1 may result from an inflammatory stimulus, for example, exposure to lipopolysaccharide (LPS), which activates cell surface toll-like receptors, namely TLR4 (Bhagat et al., 2020), and eventually results in IkB phosphorylation and NF-kB release (Kawai and Akira, 2007; Viatour et al., 2005). On the other hand, p38 is a MAPK that is involved in multiple signalling cascades including inflammatory response and is responsive to environmental stressors (Cuadrado and Nebreda, 2010; Raingeaud et al., 1995). So, the increase of these two proteins in the

nucleus of HT29 cells suggests an activation of an inflammatory response.

In N9 cells no significant increase in the nuclear translocation of either p50 or p38 was observed after 24 h of exposure to NP. This result was unexpected since N9 cells generally exhibit a strong inflammatory response to environmental stressors (Branco et al., 2022). Moreover, N9 cells did demonstrate an increase in inflammatory gene transcription after 24 h (see discussion below) which could signify that p50/p38 activation might have occurred at an earlier time-point. The lack of an effect observed with LPS exposure seems to corroborate this hypothesis since our previous experience with these cells showed that enhancement of p38 translocation happens after 6 h of exposure (Branco et al., 2022).

In line with the increased nuclear translocation of p50 in HT29 cells, we observed that exposure to NP, particularly to particles with 25 and 50 nm in diameter, upregulated TLR4 levels as seen by the western blot (Fig. 3 B). These cells constitutively express medium-low levels of TLR4 but are known to upregulate its levels upon an inflammatory stimulus (Suzuki et al., 2003). Indeed, we observed levels of TLR4 with as much as a 2-fold increase in HT29 cells exposed to NP, relative to the non-treated control (Fig. 3 B). This result is even more remarkable if we consider that N9 cells, did not up-regulate their levels following 24 h of exposure, perhaps because the basal level was already very high (Fig. 3A). In fact, LPS, the gold standard of TLR4 activators also did not promote an increase in receptor expression in N9 cells (Fig. 3).

Analysis of proinflammatory gene expression corroborates these results and suggests activation of inflammatory signalling by exposure to nanoplastics in both cell lines. Also, according to the differences observed for viability and p50 and p38 translocation, HT29 and N9 cells show different profiles of gene transcription after 24 h.

Indeed, IL-1ß increase expression in HT29 cells fits well with observations for p50 and TLR4 and suggests a canonical activation of an immune response (Jesus and Goldbach-Mansky, 2014; LaRock et al., 2016). Common activators of a TLR4/NF-kB mediated inflammatory response include LPS (Elizagaray et al., 2020), which in our HT29 model increased IL-1ß mRNA similarly to what we observed for NP. Likewise, pre-exposure of cells to a TLR4 inhibitor, prevented IL-1ß increase by both LPS and NP, which strengthens the idea that the latter induced a TLR4-mediated inflammatory response as well (Zelová and Hošek, 2013).

Furthermore, the increase in iNOS expression values in HT29 cells, suggests a typical pro-inflammatory response (Sharma et al., 2007). Indeed, increasing NO production can have beneficial microbicidal, antiviral, antiparasitic, and antitumoral activity (Kleinert and Forstermann, 2007) but at the same time contribute to free radical-mediated tissue injury in inflammatory disorders (Kolios et al., 1995).

Interestingly, we observed a great increase in IL-1ß and, particularly, iNOS mRNA levels when HT29 cells were pre-exposed to a p38 inhibitor before NP exposure (50 nm and 100 nm; 500 $\mu g.mL^{-1}$ of NP). Although intriguing, this result is in line with previous studies (Lahti et al., 2006) suggesting that inhibition of p38 MAPK leads to iNOS mRNA stabilization and increased iNOS and NO production by a JNK-mediated mechanism.

The response of N9 microglia cells to exposure to NP was quite different. As shown, these cells have a high basal level of TLR4 (Fig. 3 A) and are promptly activated by exposure to TLR4-receptor agonists, such as LPS, as seen here - by the considerable increase in IL-1ß, iNOS and TNF-α mRNA - and reported elsewhere (Vaure and Liu, 2014). Unlike with HT29 cells, upon exposure of N9 cells for 24 h to NP we did not observe any significant change in the nuclear levels of p50 and p38 (Fig. 2) or in the overall expression of TLR4 (Fig. 3B). Nevertheless, IL-1ß and iNOS mRNA levels were significantly increased by exposure to 25 $\mu g.mL^{-1}$ of NP of all sizes, so inflammatory signalling was definitely present. Indeed, in N9 cells, pre-exposure to either the TLR4 or the p38 inhibitor hindered IL-1ß and iNOS transcription (Fig. 5 A-D), thus demonstrating that these pathways are in fact involved in the inflammatory response of these cells to NP.

TNF-α mRNA was only increased in N9 cells exposed to the highest concentration of 50 nm NP (Fig. 5). Increased levels of this cytokine are normally associated to an advanced stage of inflammation. This may explain why we observed a greater effect of NP over N9 viability (Fig. 1), since TNF-α is known to activate several kinases that induce cell death (Kim et al., 2010). Still, this result lacks consistency throughout the exposure groups to allow the drawing of major conclusions. Most interestingly, the increase in TNF-α mRNA was not suppressed by pre-exposure of cells to the TLR4 inhibitor, suggesting another regulatory pathway. In agreement, p38 inhibition completely prevented the increase in TNF-α mRNA (Fig. 5 F).

5. Conclusions

Our findings demonstrate that nanoplastics induce inflammatory signalling; however, the specific mechanisms and response kinetics may vary depending on cell type and the intricate interplay of different signalling pathways. For instance, in HT29 cells, an intestinal cellular model, the notorious upregulation of TLR4 levels and p50 nuclear translocation suggest that this pathway plays a main role in inflammation. Yet, inhibiting this pathway did not consistently reduce pro-inflammatory gene transcription, implying the involvement of other factors such as p38 in the inflammatory response.

The importance of TLR4 was further emphasized as its inhibition substantially reduced IL-1ß and iNOS transcription in N9 microglia cells exposed to nanoplastics.

Moreover, N9 cells exhibited a more pronounced response, including reduced viability and cytokine expression, suggesting that nanoplastics may disrupt tissue homeostasis by activating resident macrophages. Since IL-1ß and iNOS have links to immune system dysregulation and inflammation-mediated carcinogenesis, it is imperative to conduct further research to elucidate their involvement in nanoplastic-induced intestinal and tissue inflammation.

Furthermore, the absence of knowledge concerning the internal dose of nanoplastics within biological systems hinders the accurate extrapolation of the physiological significance of these mechanisms.

It is important to emphasize that the results presented herein show occasional significant variability between replicates which in our assessment may be attributed to the propensity of NP to aggregate in culture medium, as previously discussed.

Nevertheless, it is evident from our data that polystyrene nanoplastics are by no means innocuous regarding inflammatory effects.

Funding

This research was supported by Fundação para a Ciência e Tecnologia, I.P, through: the Ph.D grant (SFRH/BD/144333/2019), JA; Norma Transitória - DL57/2016/CP1376/CT002, VB; through the Scientific Employment Stimulus - Institutional Call (CEECINST/00102/2018), MM; Nanoplastox Project – Nanoplastic Toxicity: from gut inflammation to systemic effects (2022.04884. PTDC); PAHMIX project - Mixtures of Environmental Carcinogens: a molecular approach to improve environmental risk assessment strategies (PTDC/CTA-AMB/29173/2017); MARE - Marine and Environmental Sciences Centre Strategic Project (UIDB/04292/2020), Associate Laboratory ARNET (LA/P/0069/2020) and iMed. ULisboa's Strategic Project (UID/DTP/04138/2020).

Credit authorship contribution statement

Joana Antunes: Writing – original draft, Formal analysis, Investigation. **Paula Sobral:** Resources, Writing – review & editing, Funding acquisition. **Marta Martins**: Conceptualization, Methodology, Validation, Resources, Writing – review & editing, Supervision, Project administration, Funding acquisition. **Vasco Branco**: Conceptualization,

Methodology, Validation, Resources, Writing – review & editing, Supervision, Project administration, Funding acquisition.

Declaration of Competing Interest

The authors declare that they have no known competing financial interests or personal relationships that could have appeared to influence the work reported in this paper.

Data Availability

Data will be made available on request.

Acknowledgements

The authors acknowledge Isabella Bramatti, Beatriz Matos and Neusa Figueiredo from the Marine and Environmental Sciences Centre and Carolina Carola Alfenim from University of Lisbon for their important assistance. Thanks is due to Katherine Mahoney, for revising the text. The authors acknowledge iMed.ULisboa, Faculty of Pharmacy, University of Lisbon for providing the cells tested in the present study.

Appendix A. Supporting information

Supplementary data associated with this article can be found in the online version at doi:10.1016/j.etap.2023.104298.

References

Aljabali, A.A., Obeid, M.A., Bashatwah, R.M., Serrano-Aroca, Á., Mishra, V., Mishra, Y., El-Tanani, M., Hromić-Jahjefendić, A., Kapoor, D.N., Goyal, R., Naikoo, G.A., Tambuwala, M.M., 2023. Nanomaterials and their impact on the immune system. Int. J. Mol. Sci. Vol. 24 (Issue 3) https://doi.org/10.3390/ijms24032008.

Bacher, S., Meier-Soelch, J., Kracht, M., Schmitz, M.L., 2021. Regulation of transcription factor nf-κb in its natural habitat: the nucleus. Cells Vol. 10 (Issue 4). https://doi.org/10.3390/cells10040753.

Bhagat, J., Zang, L., Nishimura, N., Shimada, Y., 2020. Zebrafish: an emerging model to study microplastic and nanoplastic toxicity. In: Science of the Total Environment, Vol. 728. Elsevier B.V. https://doi.org/10.1016/j.scitotenv.2020.138707.

Bonanomi, M., Salmistraro, N., Porro, D., Pinsino, A., Colangelo, A.M., Gaglio, D., 2022. Polystyrene micro and nano-particles induce metabolic rewiring in normal human colon cells: a risk factor for human health. Chemosphere 303. https://doi.org/10.1016/j.chemosphere.2022.134947.

Botterell, Z.L.R., Beaumont, N., Dorrington, T., Steinke, M., Thompson, R.C., Lindeque, P. K., 2019. Bioavailability and effects of microplastics on marine zooplankton: a review. Environ. Pollut. 245 (2019), 98–110. https://doi.org/10.1016/j.envpol.2018.10.065.

Bouwmeester, H., Hollman, P.C.H., Peters, R.J.B., 2015. Potential health impact of environmentally released micro- and nanoplastics in the human food production chain: experiences from nanotoxicology. Environ. Sci. Technol. 49 (15), 8932–8947. https://doi.org/10.1021/acs.est.5b01090.

Branco, V., Coppo, L., Aschner, M., Carvalho, C., 2022. N-acetylcysteine or sodium selenite prevent the p38-mediated production of proinflammatory cytokines by microglia during exposure to mercury (II). Toxics 10 (8). https://doi.org/10.3390/toxics10080433.

Carvalho, C.M.L., Chew, E.H., Hashemy, S.I., Lu, J., Holmgren, A., 2008. Inhibition of the human thioredoxin system: a molecular mechanism of mercury toxicity. J. Biol. Chem. 283 (18), 11913–11923. https://doi.org/10.1074/jbc.M710133200.

Cuadrado, A., Nebreda, A.R., 2010. Mechanisms and functions of p38 MAPK signalling. In. Biochemical Journal (Vol. 429, Issue 3,, 403–417. https://doi.org/10.1042/BJ20100323.

Du, J., Qv, W., Niu, Y., Qv, M., Jin, K., Xie, J., Li, Z., 2022. Nanoplastic pollution inhibits stream leaf decomposition through modulating microbial metabolic activity and fungal community structure. Journal of Hazardous Materials 424. https://doi.org/10.1016/j.jhazmat.2021.127392.

El Hadri, H., Gigault, J., Maxit, B., Grassl, B., Reynaud, S., 2020. Nanoplastic from mechanically degraded primary and secondary microplastics for environmental assessments. NanoImpact 17 (February), 100206. https://doi.org/10.1016/j.impact.2019.100206.

Elizagaray, M.L., Gomes, M.T.R., Guimaraes, E.S., Rumbo, M., Hozbor, D.F., Oliveira, S. C., Moreno, G., 2020. Canonical and non-canonical inflammasome activation by outer membrane vesicles derived from bordetella pertussis. Front. Immunol. 11 https://doi.org/10.3389/fimmu.2020.01879.

European Commission, 2022. (n.d.). EUROPEAN COMMISSION, 2022. https://doi.org/10.2788/36237.

Ferreira, V., Figueiredo, J., Martins, R., Sushkova, A., Maia, F., Calado, R., Tedim, J., Loureiro, S., 2023. Characterization and Behaviour of Silica Engineered Nanocontainers in Low and High Ionic Strength Media. Nanomaterials 13 (11). https://doi.org/10.3390/nano13111738.

Gopinath, M., Saranya, Shanmugam Vijayakumar, V., Meera, M.M., Ruprekha, S., Kunal, R., Pranay, A., Thomas, J., Mukherjee, A., Chandrasekaran, N. Assessment on interactive prospectives of nanoplastics with plasma proteins and the toxicological impacts of virgin, coronated and environmentally released-nanoplastics. https://doi.org/10.1038/s41598–019-45139–6.

Haldar, S., Yhome, N., Muralidaran, Y., Rajagopal, S., Mishra, P., 2023. Nanoplastics Toxicity Specific to Liver in Inducing Metabolic Dysfunction—A Comprehensive Review. Genes (Vol. 14, Issue 3). MDPI.. https://doi.org/10.3390/genes14030590.

Han, S., Bang, J., Choi, D., Hwang, J., Kim, T., Oh, Y., Hwang, Y., Choi, J., Hong, J., 2020. Surface pattern analysis of microplastics and their impact on human-derived cells. ACS Appl. Polym. Mater. 2 (11), 4541–4550. https://doi.org/10.1021/acsapm.0c00645.

Han, S.W., Choi, J., Ryu, K.Y., 2024. Recent progress and future directions of the research on nanoplastic-induced neurotoxicity. In: Neural Regeneration Research. Wolters Kluwer Medknow Publications, pp. 331–335. https://doi.org/10.4103/1673-5374.379016.

Hazeem, L.J., Yesilay, G., Bououdina, M., Perna, S., Cetin, D., Suludere, Z., Barras, A., Boukherroub, R., 2020. Investigation of the toxic effects of different polystyrene micro-and nanoplastics on microalgae Chlorella vulgaris by analysis of cell viability, pigment content, oxidative stress and ultrastructural changes. Mar. Pollut. Bull. 156 https://doi.org/10.1016/j.marpolbul.2020.111278.

He, Y., Li, J., Chen, J., Miao, X., Li, G., He, Q., Xu, H., Li, H., Wei, Y., 2020. Cytotoxic effects of polystyrene nanoplastics with different surface functionalization on human HepG2 cells. Sci. Total Environ. 723 https://doi.org/10.1016/j.scitotenv.2020.138180.

Hwang, J., Choi, D., Han, S., Jung, S.Y., Choi, J., Hong, J., 2020. Potential toxicity of polystyrene microplastic particles. Sci. Rep. 10 (1) https://doi.org/10.1038/s41598-020-64464-9.

Jesus, A.A., Goldbach-Mansky, R., 2014. IL-1 blockade in autoinflammatory syndromes. Annu. Rev. Med. 65 (1), 223–244. https://doi.org/10.1146/annurev-med-061512-150641.

Jewett, E., Arnott, G., Connolly, L., Vasudevan, N., Kevei, E., 2022. Microplastics and Their Impact on Reproduction—Can we Learn From the C. elegans Model?. In: *Frontiers in Toxicology*, (Vol. 4).. Frontiers Media S.A. https://doi.org/10.3389/ftox.2022.748912.

Jung, B.K., Han, S.W., Park, S.H., Bae, J.S., Choi, J., Ryu, K.Y., 2020. Neurotoxic potential of polystyrene nanoplastics in primary cells originating from mouse brain. NeuroToxicology 81, 189–196. https://doi.org/10.1016/j.neuro.2020.10.008.

Kawai, T., Akira, S., 2007. Signaling to NF-κB by toll-like receptors. Trends Mol. Med. Vol. 13 (Issue 11), 460–469. https://doi.org/10.1016/j.molmed.2007.09.002.

Kihara, S., Ashenden, A., Kaur, M., Glasson, J., Ghosh, S., van der Heijden, N., Brooks, A. E.S., Mata, J.P., Holt, S., Domigan, L.J., Köper, I., McGillivray, D.J., 2021. Cellular interactions with polystyrene nanoplastics—the role of particle size and protein corona. Biointerphases 16 (4). https://doi.org/10.1116/6.0001124.

Kim, J.J., Lee, S.B., Park, J.K., Yoo, Y.D., 2010. TNF-α-induced ROS production triggering apoptosis is directly linked to Romo1 and Bcl-XL. Cell Death Differ. 17 (9), 1420–1434. https://doi.org/10.1038/cdd.2010.19.

Kleinert, H., Forstermann, U., 2007. Inducible nitric oxide synthase. XPharm: Compr. Pharmacol. Ref. 1–12. https://doi.org/10.1016/B978-008055232-3.60509-4.

Kolios, G., Brown, Z., Robson, R.L., Robertson, tDuncan A., & Westwick, John, 1995. Inducible nitric oxide synthase activity and expression in a human colonic epithelial cell line, HT-29.

Lahti, A., Sareila, O., Kankaanranta, H., Moilanen, E., 2006. Inhibition of p38 mitogen-activated protein kinase enhances c-Jun N-terminal kinase activity: implication in inducible nitric oxide synthase expression. BMC Pharmacol. 6 https://doi.org/10.1186/1471-2210-6-5.

LaRock, C.N., Todd, J., LaRock, D.L., Olson, J., O'Donoghue, A.J., Robertson, A.A.B., Cooper, M.A., Hoffman, H.M., Nizet, V., 2016. IL-1b is an innate immune sensor of microbial proteolysis. Sci. Immunol. 1 (2) https://doi.org/10.1126/sciimmunol.aah3539.

Larue, C., Sarret, G., Castillo-Michel, H., Pradas del Real, A.E., 2021. A Critical Review on the Impacts of Nanoplastics and Microplastics on Aquatic and Terrestrial Photosynthetic Organisms. Small (Vol. 17, Issue 20).. https://doi.org/10.1002/smll.202005834.

Li, Y., Xu, M., Zhang, Z., Halimu, G., Li, Y., Li, Y., Gu, W., Zhang, B., Wang, X., 2022. In vitro study on the toxicity of nanoplastics with different charges to murine splenic lymphocytes. J. Hazard. Mater. 424 https://doi.org/10.1016/j.jhazmat.2021.127508.

Liu, T., Zhang, L., Joo, D., Sun, S.C., 2017. NF-κB signaling in inflammation. In: Signal Transduction and Targeted Therapy, Vol. 2. Springer Nature. https://doi.org/10.1038/sigtrans.2017.23.

Livak, K.J., Schmittgen, T.D., 2001. Analysis of relative gene expression data using real-time quantitative PCR and the 2-ΔΔCT method. Methods 25 (4), 402–408. https://doi.org/10.1006/meth.2001.1262.

Llorca, M., Farré, M., 2021. Current insights into potential effects of micro-nanoplastics on human health by in-vitro tests. Front. Toxicol. 3 https://doi.org/10.3389/ftox.2021.752140.

Mattsson, K., Hansson, L.A., Cedervall, T., 2015. Nano-plastics in the aquatic environment. In: Environmental Sciences: Processes and Impacts, Vol. 17. Royal Society of Chemistry, pp. 1712–1721. https://doi.org/10.1039/c5em00227c.

Oliveira, Y.M., Vernin, N.S., Bila, D.M., Marques, M., Tavares, F.W., 2022. Pollution caused by nanoplastics: adverse effects and mechanisms of interaction via molecular simulation. PeerJ 10. https://doi.org/10.7717/peerj.13618.

Pabortsava, K., Lampitt, R.S., 2020. High concentrations of plastic hidden beneath the surface of the Atlantic ocean. Nat. Commun. 11 (1) https://doi.org/10.1038/s41467-020-17932-9.

Palmer, J., Herat, S., 2021. Ecotoxicity of Microplastic Pollutants to Marine Organisms: a Systematic Review. In Water. In: Air, and Soil Pollution, (Vol. 232, Issue 5). Springer Science and Business Media Deutschland GmbH. https://doi.org/10.1007/s11270-021-05155-7.

PlasticsEurope, 2022. (n.d.). Available at: https://plasticseurope.org October 1st 2023.

Poltorak, A., He, X., Smirnova, I., Liu, M.Y., van Huffel, C., Du, X., Birdwell, D., Alejos, E., Silva, M., Galanos, C., Freudenberg, M., Ricciardi-Castagnoli, P., Layton, B., Beutler, B., 1998. Defective LPS signaling in C3H/HeJ and C57BL/10ScCr mice: mutations in Tlr4 gene. Science 282 (5396), 2085–2088. https://doi.org/10.1126/science.282.5396.2085.

Ragnarsdóttir, O., Abdallah, M.A.E., Harrad, S., 2022. Dermal uptake: an important pathway of human exposure to perfluoroalkyl substances?. In: Environmental Pollution, Vol. 307 Elsevier Ltd. https://doi.org/10.1016/j.envpol.2022.119478.

Raingeaud, J., Gupta, S., Rogers, J.S., Dickens, M., Han, J., Ulevitch, R.J., Davis, R.J., 1995. Pro-inflammatory cytokines and environmental stress cause p38 mitogen-activated protein kinase activation by dual phosphorylation on tyrosine and threonine. J. Biol. Chem. 270 (13), 7420–7426. https://doi.org/10.1074/jbc.270.13.7420.

Revel, M., Châtel, A., Mouneyrac, C., 2018. Micro(nano)plastics: a threat to human health?. In: Current Opinion in Environmental Science and Health, Vol. 1 Elsevier B. V., pp. 17–23. https://doi.org/10.1016/j.coesh.2017.10.003

Sharif, O., Bolshakov, V.N., Raines, S., Newham, P., Perkins, N.D., 2007. Transcriptional profiling of the LPS induced NF-κB response in macrophages. BMC Immunol. 8 https://doi.org/10.1186/1471-2172-8-1.

Sharma, J.N., Al-Omran, A., Parvathy, S.S., 2007. Role of nitric oxide in inflammatory diseases. InflAmmopharmacology 15, 252–259. https://doi.org/10.1007/s10787-007-0013-x.

Suzuki, M., Hisamatsu, T., Podolsky, D.K., 2003. Gamma interferon augments the intracellular pathway for lipopolysaccharide (LPS) recognition in human intestinal epithelial cells through coordinated up-regulation of LPS uptake and expression of the intracellular Toll-like receptor 4-MD-2 complex. Infect. Immun. 71 (6), 3503–3511. https://doi.org/10.1128/IAI.71.6.3503-3511.2003.

Teles, M., Balasch, J. C., Oliveira, M., Sardans, J., Peñuelas, J., 2020. Insights into nanoplastics effects on human health. In: Science Bulletin, (Vol. 65, Issue 23,. Elsevier B.V, pp. 1966–1969. https://doi.org/10.1016/j.scib.2020.08.003.

Vaure C, Liu Y. A comparative review of toll-like receptor 4 expression and functionality in different animal species. Front Immunol. 2014 Jul 10;5:316. doi: 10.3389/fimmu.2014.00316.

Vezza, T., Rodríguez-Nogales, A., Algieri, F., Utrilla, M.P., Rodriguez-Cabezas, M.E., Galvez, J., 2016. Flavonoids in inflammatory bowel disease: a review. Nutrients Vol. 8 (Issue 4). https://doi.org/10.3390/nu8040211.

Viatour, P., Merville, M.P., Bours, V., Chariot, A., 2005. Phosphorylation of NF-κB and IκB proteins: implications in cancer and inflammation. Trends Biochem. Sci. Vol. 30 (Issue 1), 43–52. https://doi.org/10.1016/j.tibs.2004.11.009.

Wang, W., Weng, J., Yu, L., Huang, Q., Jiang, Y., Guo, X., 2018. Role of TLR4-p38 MAPK-Hsp27 signal pathway in LPS-induced pulmonary epithelial hyperpermeability. BMC Pulm. Med. 18 (1) https://doi.org/10.1186/s12890-018-0735-0.

Whitaker, R.H., Cook, J.G., 2021. Stress relief techniques: p38 MAPK determines the balance of cell cycle and apoptosis pathways. biomolecules. https://doi.org/10.3390/biom11101444.

Yee, M.S.L., Hii, L.W., Looi, C.K., Lim, W.M., Wong, S.F., Kok, Y.Y., Tan, B.K., Wong, C. Y., Leong, C.O., 2021. Impact of microplastics and nanoplastics on human health. Nanomaterials Vol. 11 (Issue 2), 1–23. https://doi.org/10.3390/nano11020496.

Zbinden-Foncea, H., Raymackers, J.M., Deldicque, L., Renard, P., Francaux, M., 2012. TLR2 and TLR4 activate p38 MAPK and JNK during endurance exercise in skeletal muscle. Med. Sci. Sports Exerc. 44 (8), 1463–1472. https://doi.org/10.1249/MSS.0b013e31824e0d5d.

Zelová, H., Hošek, J., 2013. TNF-α signalling and inflammation: interactions between old acquaintances. Inflamm. Res. Vol. 62 (Issue 7), 641–651. https://doi.org/10.1007/s00011-013-0633-0.

Zhou, Y., He, G., Jiang, H., Pan, K., Liu, W., 2023. Nanoplastics induces oxidative stress and triggers lysosome-associated immune-defensive cell death in the earthworm Eisenia fetida. Environ. Int. 174 https://doi.org/10.1016/j.envint.2023.107899.

Glossary

ATCC: American Type Culture Collection
BSA: bovine serum albumin
cDNA: complementary DNA
EDTA: Ethylenediaminetetraacetic acid
EGTA: ethylene glycol-bis(β-aminoethyl ether)-N,N,N′,N′-tetraacetic acid
FBS: Fetal bovine serum
GAPDH: Glyceraldehyde 3-phosphate dehydrogenase
HEPES: 4-(2-hydroxyethyl)− 1-piperazineethanesulfonic acid
HT29 cells: human colorectal adenocarcinoma cells
IL-1: Interleukin 1
IL-1β: Interleukin 1 beta
iNOS: inducible nitric oxide synthase
iq.r: interquartile range
LPS: lipopolysaccharide
mM: millimolar concentration
MTT: 3-(4,5-dimethylthiazol-2-yl)− 2,5-diphenyltetrazolium bromide
N9 cells: mouse microglial cells
NP: nanoplastics
p50 NF-KB: nuclear factor kappa light chain enhancer of activated B cells
p38 MAPK: Mitogen-activated protein kinase
PBS: phosphate buffered saline
PCR: polymerase chain reaction
PS: polystyrene
RPMI: Roswell Park Memorial Institute
qPCR: Real-time polymerase chain reaction
SDS-PAGE: electrophoresis with acrylamide gel
TLR4: toll-like receptor 4
TNF-α: Tumor necrosis factor alpha
Tris-Cl: Tris (triphenylphosphine)rhodium (I) chloride